VOL. 23, NO. 2, 2024, 116-122
elektrika.utm.my
ISSN 0128-4428

ELEKTRIKA
Journal of Electrical Engineering

Regenerative Braking Conscious Rule-Based Energy Management Strategy for Semi-Active Hybrid Energy Storage Systems for Electric Vehicles

Mohammad Al Takrouri[1], **Nik Rumzi Nik Idris**[1], **Mohd Junaidi Abdul Aziz**[1*], **Razman Ayop**[1], and **Rozana Alik**[1]

[1]Faculty of Electrical Engineering, Universiti Teknologi Malaysia, 81310 UTM Skudai, Johor, Malaysia.

[*]Corresponding author: junaidi@utm.my

Abstract: Hybrid Energy Storage Systems (HESS) function as a solution to extend the lifespan of battery packs by maintaining a low charge/discharge rate. The integration of HESS in electric vehicles (EVs) is facilitated by supercapacitors (SC), known for their safe operation even under harsh conditions. The widely adopted rule-based power follower energy management strategy (EMS) is employed to control and restrict battery discharge within a defined range with SC support. Additionally, it charges the SC to accommodate regenerative energy, but it often neglects exploring the SC voltage set reference. This study investigates the SC voltage reference point and introduces a method to generate the reference point by equating the SC energy with the available kinetic energy in the moving vehicle. The proposed method was simulated and compared against the benchmark method using a portion of the medium segment Worldwide Harmonized Light Vehicles Test Procedure (WLTP) driving cycle. The results demonstrate a more stable discharge power for the battery bank, accompanied by improvements in battery voltage stability. The root mean square (RMS) battery current values were found to be 43.68 A and 42.92 A for the benchmarked and proposed methods, respectively, indicating a slight improvement of about 1%. Furthermore, the proposed method reduces the voltage deviation from 2.73% to about 2.57%, showcasing an additional positive outcome. These findings suggest that dynamically adjusting the SC voltage based on kinetic energy can enhance battery life and stability in EVs, offering a promising direction for future research and development of EMS.

Keywords: Hybrid Energy Storage System, Regenerative Braking, Supercapacitor, Supercapacitor voltage reference

Article History: received 28 December 2023; accepted 19 July 2024; published 29 August 2024

1. INTRODUCTION

Electric vehicles (EVs) are rapidly gaining traction as a promising solution to reduce carbon emissions and transform the transportation sector. The global shift towards EV adoption is evident in various countries due to political and environmental reasons. A reported showed that the EV sales projections for 2030 more than doubled, growing from the initial estimate of 21% to 53% [1]. Nevertheless, it is crucial to note that EVs may not yield efficiency improvements over traditional gasoline cars if their electricity source originates from traditional coal-fired power plants [2]. Despite this challenge, the adoption of EVs presents an opportunity to diversify power generation into renewable energy sources. This shift has the potential to make substantial contributions to Sustainable Development Goals (SDGs), particularly SDG 13: climate action and SDG 7: affordable and clean energy [3]. One of the EV adoption hurdles is the limited lifespan of its lithium-ion batteries, which is affected by many factors such as charge/discharge rate, temperature and depth of discharge (DoD) [4]. One of the innovative solutions to reduce these effects is to implement a HESS. The main idea of HESS is to couple the high energy density energy storage device (ESD), such as a lithium-ion battery pack, with high power density alternative ESDs, such as superconducting magnetic, flywheels, and supercapacitors (SCs).

Superconducting magnetic offers excellent storage capability. However, it is mainly used for stationary applications due to its vulnerability to temperature variations [5]. Flywheels, on the other hand, are excellent at storing energy up to 100Wh/kg; however, they come with a high discharge rate of about 20% per hour, in addition to the nuisance of maintenance of the moving parts compared to static energy storage systems [6], which leaves us with the SCs. SCs are one of the attractive candidates to be used inside moving vehicles where their inherent solid-state structure makes them safe. In addition, SC typical graphene cell can have a specific energy reach up to $11.1 Wh/kg$ and specific power of about $20 kW/kg$ [7]. There are multiple circuit topologies to incorporate a SC bank in an EV.

The topologies in HESS refer to the placement of the components in the organization of electrical circuits. The “active” refers to having the ability to control the power

flow in the circuit, which requires the usage of a direct current (DC)-DC converter. The current work opts for the semi-active SC/battery topology, given its notable advantages. This topology is widely employed [8] and stands out for its controllability, extensive range of SC voltage and utilization, and superior efficiency [9]. In order to activate the HESS, reference values must be acquired. The references must be appropriate to provide a suitable power split between the two or more energy storage systems while respecting the limitations of each device and ensuring superior performance. Many algorithms are being developed and investigated by researchers, which can be categorized into two main divisions [10]: rule-based and optimization-based.

Load follower [11] or power follower is a rule-based energy management strategy (EMS) that splits the demand power between the storage devices based on an "if-then" algorithm using system input measurements such as state of charge (SOC), power demand, and current values. One of the demonstrations of the power follower EMS is an experiment done by [12], which achieved a reduction of the battery peak current of about 40%. The issue with this method is that the battery still experiences a high-frequency current value in addition to a lack of optimization. However, due to its robustness and simplicity, many commercial hybrid vehicles such as Toyota Prius and Honda Insight, uses this method [13].

Optimization-based control algorithms for EMSs are based on the formulation of the objective function and finding the optimum solution while respecting the system constraints. One of the key challenges of the optimization-based control algorithm is the difficulty of applying it online due to the high cost of computational, memory resources, and the requirement of the future load demand to be known or predicted. However, many optimization-based EMSs have been adapted to be applied online with the sacrifice of optimal performance. A model predictive control EMS was tested [14] for the EMS assuming a constant future in order to compare it to other rule-based EMSs. The comparative study found that the model predictive control (MPC) EMS underperformed in terms of battery degradation due to the accumulation of prediction errors.

Due to the ongoing relevancy of the power-follower strategy [15], [16], there is still room for improvement, specifically for the SC voltage, as it is allowed to vary between 50% to 100% of that of the semi-active HESS. In the classical power follower strategy, the SC reference voltage (v_{sc}^*) was allowed to follow a specific trend for a given vehicle [11] which is proportional to the vehicle speed. The selection of the reference point for the SC voltage or its SOC is not the focal point of many of the HESS control systems. However, various methods exist; most commonly, the SC voltage reference is set at a constant middle point between the maximum and minimum voltage [17]–[20]. Meanwhile, Song *et al.* [14] kept the SC voltage reference at 90% of its rated maximum value, giving priority to the SC to support the upcoming acceleration power demand. Choi *et al.* [21] implemented a more conscious approach to implement a varied SC voltage reference based on the energy balance between the powertrain and SC energy, which includes a piecewise function that takes into account the braking energy split between the mechanical and regenerative braking. In their work, the obtained SC voltage reference was used as input to a convex optimization problem to calculate the optimum power for the HESS.

Hence, the objective of this paper is to refine the method of obtaining the SC voltage reference in the power follower EMS [11] to account for the available kinetic or absence of kinetic energy in the rotational mass of the vehicle. This estimation attempt is tested on a simple but robust EMS without a complex optimization method, as in [21]. The validation is conducted through a simulation comparison between two methods of obtaining SC voltage reference used in a rule-based power follower EMS.

This paper is structured into five sections for a comprehensive exploration of the proposal. Section 2 details the system description, emphasizing the semi-active SC/battery topology model and its control structure. In Section 3, the novel SC voltage reference strategy is introduced in addition to its incorporation to the EMS. Section 4 presents the simulation results. Finally, the conclusion remarks are in section 5. This concise organization ensures a focused examination of HESS integration and energy management strategies for enhanced EV performance.

2. SYSTEM DESCRIPTION

From the control perspective, enabling the HESS requires two main levels, as shown in Figure 1. The first level, which is referred to as upper-level EMS, provides the reference points, for instant SC current reference, i_{sc}^*, that provide the effective power split between the energy storage devices. The EMS utilizes the system measurement, such as battery voltage, v_b, and SC voltage, v_{sc}. In addition, to SC voltage reference v_{sc}^*. The second level, or the underlying level, is the control loop that tracks these reference points, which is enforced by the power converters via the switching signal, S. For full-active and semi-active SC/B topologies, where the SC voltage is not fixed at the DC bus voltage, the SC voltage reference point should be obtained and tracked.

The rule-based power follower EMS has simplicity as one of its features, where the SC voltage regulator is merged with the energy management strategy to decrease the number of regulators in the systems. Resulting in the system control block diagram in Figure 2.

2.1 System Model

The widely used semi-active SC/battery topology is selected in this work due to its advantages, as discussed in

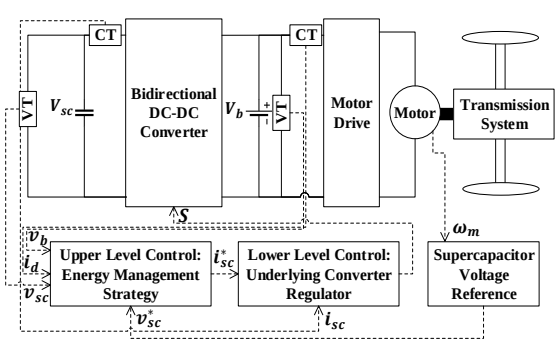

Figure 1. Hybrid energy storage system for vehicular application and its control structure.

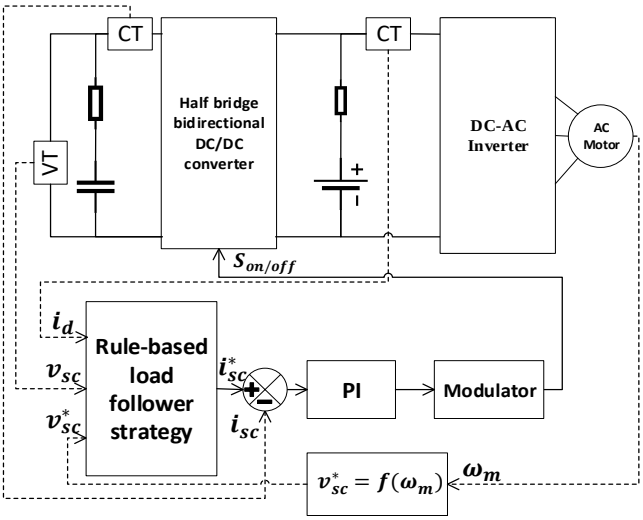

Figure 2. Semi-active SC/battery hybrid energy storage system control system block diagram.

the previous section. Since the focal point of this paper is to develop and compare between EMS control strategies, the bidirectional DC-DC converter is assumed to be ideal in addition to the simplified models of the battery bank and SC packs. Figure 3 shows the simplified model of the HESS, consisting of a battery, SC, and the propulsion system, which are modelled by rint models for the energy storage devices and a current source for the demand load. The battery pack and SC bank are represented by two equivalent lumped components with equivalent series resistances r_b and r_{sc}, respectively, in addition to the ideal voltage sources v_b and v_{sc}. Finally, the DC-DC two-quadrant bidirectional converter is represented by two IGBT power electronic switches, T_1 and T_2; an inductor (L) with its equivalent resistance r_L; and a smoothing capacitor C_f, which together form the half-bridge bidirectional DC-DC converter.

The complementary operation of the bidirectional converter maintains the continuous current mode, ensuring the demand power flow in the HESS topology aligns with the energy conservation principles. This entails the net sum of power flowing between the battery pack and the SC bank in the hybrid energy storage system as in equation (1):

$$p_d = p_b + p_{sc} \tag{1}$$

Where p_d, p_b, and p_{sc} are the powers of the demand load, battery pack, and SC bank. In this topology, the battery pack is the main energy storage system, with the SC bank acting as a supporting energy storage device. The goal of the upper EMS (discussed in section 3.2) is to obtain the value of p_{sc}^* and enforce it via lower-level regulators.

Tuning the lower-level controller, which in this case is a PI regulator, requires obtaining the small signal model of the circuit in Figure 3. Since the half-bridge converter operates according to the duty cycle, the time period accounted for the on state is $d(t)$, while $\acute{d} = 1 - d(t)$ refers to the complement of the duty cycle. Hence, the average state space model of the circuit is shown in equation (2):

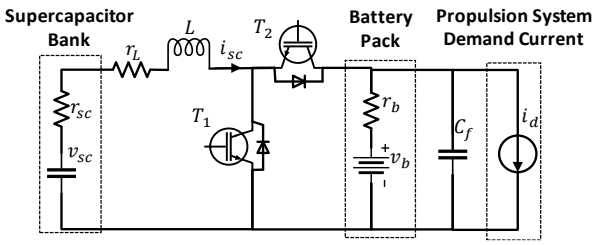

Figure 3. Equivalent circuit of the hybrid energy storage system

$$\begin{aligned} \dot{\boldsymbol{x}}(\boldsymbol{t}) &= \left[\mathbf{A_1}d(t) + \mathbf{A_2}\hat{d}(t)\right]\boldsymbol{x}(\boldsymbol{t}) + \\ &\left[\mathbf{B_1}d + \mathbf{B_2}\hat{d}(t)\right]u(t) \\ \boldsymbol{y}(\boldsymbol{t}) &= \left[\boldsymbol{C_1}d(t) + \boldsymbol{C_2}\hat{\mathrm{d}}(t)\right]\boldsymbol{x}(\boldsymbol{t}). \end{aligned} \tag{2}$$

Firstly, the system disturbances are neglected since they are out of the scope of this study. However, since the half-bridge converter circuit changes depending on the dual states (buck mode or boost mode), the state space representation matrices $\boldsymbol{A}$ changes. In order to distinguish between the two different system matrices, $\boldsymbol{A_1}$ is referred to as the boost mode matrix and $\boldsymbol{A_2}$ to the buck mode matrix. In the case of the rest of the parameters of the state space representation, they are fixed in both modes of operation. The derivation begins by writing the differential equation of the circuit in Figure 3. The small signal model is developed by separating the AC perturbation from the DC quiescent quantities as the following equation (3):

$$\begin{aligned} \dot{\mathbf{X}} + \dot{\tilde{\boldsymbol{x}}} &= \left[\mathbf{A_1}\left(\mathrm{D} + \tilde{d}\right) + \mathbf{A_2}\left(\acute{\mathrm{D}} - \tilde{d}\right)\right](\mathbf{X} + \tilde{\boldsymbol{x}}) + \\ &\left[\mathbf{B_1}\left(\mathrm{D} + \tilde{d}\right) + \mathbf{B_2}\left(\acute{\mathrm{D}} - \tilde{d}\right)\right](\mathrm{U} + \tilde{u}) \\ \mathbf{Y} + \tilde{\boldsymbol{y}} &= \left[\mathbf{C_1}\left(\mathrm{D} + \tilde{d}\right) + \mathbf{C_2}\left(\acute{\mathrm{D}} - \tilde{d}\right)\right](\mathbf{X} + \tilde{\boldsymbol{x}}). \end{aligned} \tag{3}$$

In this specific case, the output voltage is fixed by the battery, making both piecewise affine modes equal except for the differences in the matrices of $\boldsymbol{B}$. The equivalent circuit has the following parameters as shown in equation (4):

$$\begin{gathered} \boldsymbol{x}(\boldsymbol{t}) = \begin{bmatrix} i_L(t) \\ v_{sc}(t) \end{bmatrix} \\ \boldsymbol{y}(\boldsymbol{t}) = \begin{bmatrix} i_{sc}(t) \\ v_{sc}(t) \end{bmatrix} \\ U = V_b \\ \boldsymbol{A_1} = \boldsymbol{A_2} = \boldsymbol{A} = \begin{bmatrix} -\dfrac{r_L + r_{SC}}{\mathrm{L}} & \dfrac{1}{L} \\ \dfrac{1}{C_{sc}} & 0 \end{bmatrix} \\ \boldsymbol{C_1} = \boldsymbol{C_2} = \boldsymbol{C} = [1 \quad 0] \\ \boldsymbol{B_1} \neq \boldsymbol{B_2} \end{gathered} \tag{4}$$

$$\boldsymbol{B_1} = \begin{bmatrix} 0 \\ 0 \end{bmatrix}$$

$$\boldsymbol{B_2} = \begin{bmatrix} \frac{1}{L} \\ 0 \end{bmatrix}$$

Rewriting (3) while neglecting the 2nd-order perturbation, such as $\tilde{d}\tilde{x}$ due to their small contribution to the dynamics, equation (5) is obtained:

$$\begin{aligned} \dot{\tilde{x}} &= \boldsymbol{A}\tilde{x} + \boldsymbol{B}\tilde{u} + (\boldsymbol{B_1} - \boldsymbol{B_2})U\tilde{d} \\ \tilde{y} &= \boldsymbol{C}\tilde{x} \end{aligned} \tag{5}$$

The input voltage for our case is the battery voltage, and its variation is considered small enough, hence the term $\boldsymbol{B}\tilde{u}$ is neglected for simplification. Transforming the previous equation to s-domain using Laplace transformation as equation (6):

$$s\boldsymbol{X}(\boldsymbol{s}) = A\boldsymbol{X}(\boldsymbol{s}) + (\boldsymbol{B_1} - \boldsymbol{B_2})UD(s) \tag{6}$$

Solving for the transfer function consisting of the loop between the applied duty cycle to SC current, the following solution in equation (7) and (8) is found:

$$\begin{aligned} \boldsymbol{Y}(\boldsymbol{s}) &= \boldsymbol{C}\boldsymbol{X}(\boldsymbol{s}) \\ \boldsymbol{Y}(\boldsymbol{s}) &= \boldsymbol{C}[s\boldsymbol{I} - \boldsymbol{A}]^{-1}(\boldsymbol{B_1} - \boldsymbol{B_2})UD(s) \end{aligned} \tag{7}$$

$$\frac{I_{sc}(s)}{D(s)} = \boldsymbol{C}[s\boldsymbol{I} - A]^{-1}(\boldsymbol{B_1} - \boldsymbol{B_2})U \tag{8}$$

After simplification, the result is equation (9):

$$\frac{I_{sc}(s)}{D(s)} = \frac{\frac{V_b}{L}s}{s^2 + \frac{(r_{sc} + r_L)}{L}s - \frac{1}{LCsc}} \tag{9}$$

The vehicle parameter and HESS are found in TABLE 1. The system's bandwidth under control is found to be $124\ rad/s$, then the current closed-loop cutoff frequency is chosen to be $1000\ rad/s$. The phase margin is chosen $\phi_I = 50^o$.

3. HYBRID ENERGY STORAGE SYSTEM CONTROL SCHEME

This section explores the upper-level control EMS and the SC voltage reference. Initially, the discussion revolves around the proposed method for generating the SC voltage reference and its derivation. Following this, the power follower EMS is revisited, integrating the newly derived SC voltage reference into the EMS.

3.1 Supercapacitor Voltage Reference

The SC voltage reference is derived based on the conservation of energy law between the vehicle and SC bank; this is done by equating both sides as in equation (10):

$$E_{SC} = E_k \tag{10}$$

Table 1. Vehicle paramters

M_v	Vehicle gross weight (kg)	1050
$S_{v,max}$	Peak Vehicle Speed (km/h)	115
P_M	Continuous power (kW)	38
Ra	Motor equivalent resistance (Ω)	0.1113
L_a	Motor equivalent inductance (H)	$1.558 * 10^{-3}$
B	Viscous friction coefficient (Nm/rpm)	$7.032 * 10^{-3}$
J_{eq}	Equivalent inertia (kgm^2)	34.97
V_b	Battery pack rated voltage (V)	240
C_b	Battery pack capacity (kWh)	50.4
r_b	Battery pack ESR $(m\Omega)$	28
L	Bidirectional converter inductor (mH)	0.21
r_L	Bidirectional converter inductor ESR (mΩ)	20
C	Output capacitor (mF)	30
C_{sc}	Supercapacitor capacitance (F)	138.5
r_{sc}	Supercapacitor ESR $(m\Omega)$	8.8

Where E_{SC} is the stored energy in the SC, and E_k is the kinetic energy. The stored energy SC follows the basic capacitor formula in equation (11):

$$E_{SC} = \frac{1}{2}C_{SC}v_{SC}(t)^2 \tag{11}$$

Where $v_{SC}(t)$ is the SC voltage at the time instant t and C_{SC} is the total capacitance. Considering the energy available at time, t, equation (12) is obtained:

$$E_{SC} = \frac{1}{2}C_{SC}\left[V_{SC,max}^2 - v_{SC}^*(t)^2\right] \tag{12}$$

Given the available kinetic energy at a certain speed, $s(t)$, and mass, M_t, the kinetic energy is calculated using equation (13):

$$E_k = \frac{1}{2}M_{tot}s(t)^2 \tag{13}$$

To ensure both sides of the equation are equal, a factor of efficiencies that takes into account all the losses in the power train is considered, as shown in Figure 4. According to the work by Ramdan *et al*. [22], the mechanical efficiency (η_{mech}) of the Perodua Myvi Automatic is estimated to be between 85% and 95%. For the Synchronous Reluctance Internal Permanent Magnet (SRIPM) motor, the overall efficiency (η_m) ranges from 88% to 95% [23]. η_{sc} falls within the range of 95% to 98% [24]. On the other hand, the conversion efficiency (η_{con}) of the SC bank current voltage varies between 60% and 98%, based on the efficiency map [25]. However, the bidirectional converter can achieve high efficiency if the boosted voltage does not exceed three times the SC current and the operation of the SC bank is limited to 50% of its state of charge (SOC). Accounting for the total efficiency equation (14) is derived:

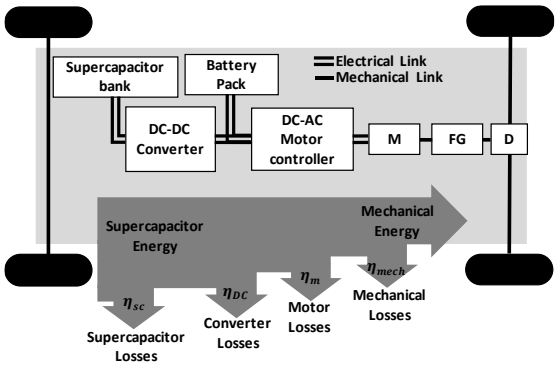

Figure 4. Electric vehicle energy flow losses

$$\eta_{\text{total}}\, C_{SC}\left[V_{SC,max}^2 - v_{SC}^*(t)^2\right] = M_V s_{V,max}^2 \qquad (14)$$

Where:

$$\eta_{\text{total}} = \eta_{\text{mech}}\,\eta_{\text{m}}\eta_{\text{con}}\eta_{\text{sc}}$$

$$= 0.95 * 0.95 * 0.98 * 0.90 = 0.80$$

Equating both equations and solving for the SC voltage, the estimated SC voltage reference is derived as in equation (15):

$$v_{sc,est}^*(t) \cong \sqrt{V_{\text{SC},max}^2 - \frac{\text{M}_\text{V} s_V^2(t)}{\eta_{\text{tot}}\,\text{C}_\text{SC}}} \qquad (15)$$

The SC voltage is limited to varying between 50% and 100% to restrict the operation of the bidirectional converter at the highest efficiency points. For the upper voltage limit, The SC voltage reference should follow the following piecewise function in equation (16):

$$v_{sc}^*(t) = \begin{cases} 0.5V_{sc,rated} & v_{sc}^*(t) < 0.5V_{sc,rated} \\ V_{sc,rated} & v_{sc}^*(t) > V_{sc,rated} \\ v_{sc,est}^*(t) & \text{otherwise} \end{cases} \qquad (16)$$

In this study, the reference $v_{sc}^*(t)$ given by (15) and (16) is compared to the original rule-based power follower EMS given by [11] as in equation (17):

$$v_{sc,carter}^*(t) = V_{sc,rated} * \sqrt{1 - \frac{3 * s_V^2(t)}{160}} \qquad (17)$$

3.2 Energy Management Strategy

To accomplish the desired implementation of the HESS, an EMS must be designed. An EMS is used to generate the SC current reference value. In this study, the practical rule-based power split strategy by Carter *et al*. [11] is utilized due to its advantages over the other energy split algorithms. The SC power reference is produced based on the algorithm, as shown in Figure 5, where the SC power reference at the time instant k referred by $p_{sc}^*(k)$ is the output of the flowchart, which is usually divided by SC voltage $\left(v_{sc}(k)\right)$ to obtain the current reference. The power split algorithm is tuned based on the threshold value of the maximum power of the demand. $\left(p_d(k)\right)$ which the battery pack can supply without imposing any additional stress referred by P_{min}. In addition, the SC is charged until it reaches its SC voltage reference $v_{sc}^*(k)$ obtain from (15) or (17) for the proposed method and for the original. In addition, other SC voltage discharging and charging limits are defined as V_{max} and V_{min} which are the SC maximum and minimum voltages.

4. SIMULATION RESULTS

The purpose of the simulation is to validate the proposed SC voltage refence method. It involves comparing the original power follow strategy of EMGs with the proposed modification in this study. The simulation uses the WLTP driving cycle. The WLTP driving cycle has a period of about 1800s. However, in this study, the period between 590s to 1022s is chosen, as shown in Figure 6, which mimics the behavior of a city-driven car with frequent braking and accelerating. The simulation is conducted using MATLAB/Simulink software and includes high-fidelity models of the battery pack, SC bank, and motor load. The focus of this study is to analyze the EMS, so details about the motor and its control are not included in this paper.

Figure 7 and Figure 8 present the simulation results for the benchmark and proposed methods, respectively. Both figures are organized similarly, with the top plot showing the vehicle speed and SOC, the middle plot showing the demand power and battery power, and the bottom plot showing the SC power and its reference. Since the power follower EMS does not have a regulated SC voltage, the SC reference voltage is not tracked but rather treated as the recommended value for charging the SC bank. The proposed method reaches the minimum SC SOC reference at around 60 km/h, while the benchmark method reaches it at about 45 km/h. This difference in speed results in a more dynamic SOC for the proposed method. The consequence of this can be observed in the time period between 300-350s, where the SC is depleted to support acceleration power in the proposed method due to the suggested SOC reference voltage being close to the lower limit allowed by the bidirectional converter. This is not always apparent but can be noticed during this specific time period of the driving cycle. The voltage stability of the system is also affected by these differences. Figure 9 shows that the benchmark control system experiences several voltage spikes compared to the proposed system. This will directly reflect on the motor efficiency [9].

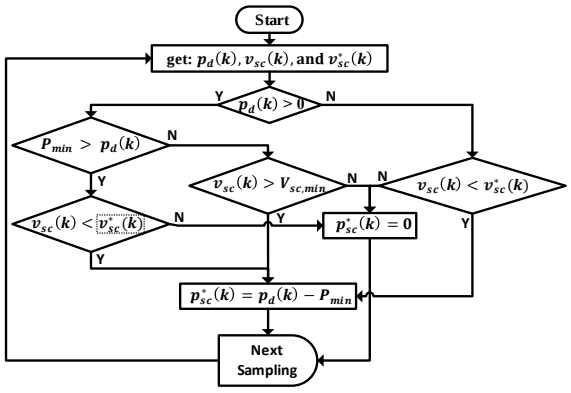

Figure 5. Rule-based power follower energy management strategy [11]

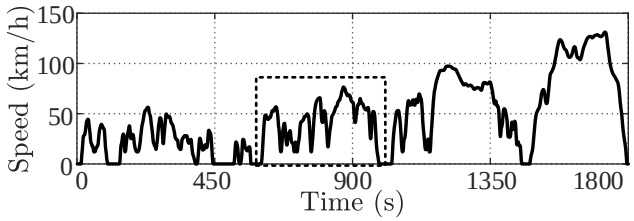

Figure 6. Worldwide Harmonised Light Vehicle Test Procedure driving cycle and selected portion for testing

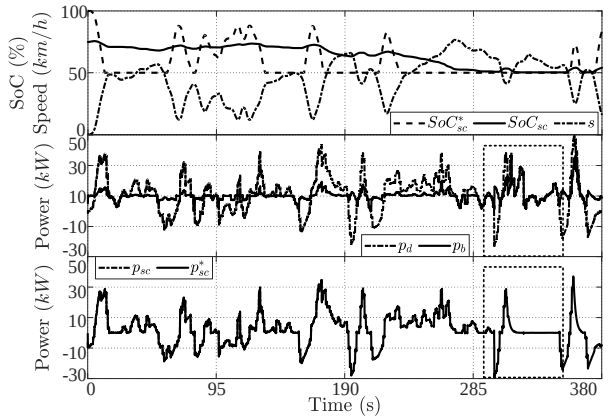

Figure 7. simulation results for benchmark method showing vehicle speed, supercapacitor state of charge and its reference (top), instantaneous powers for demand, battery, SC, and its reference

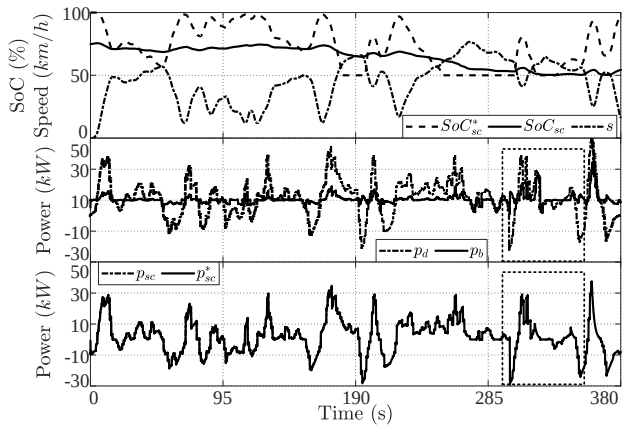

Figure 8. simulation results for the proposed method showing vehicle speed, supercapacitor state of charge and its reference (top), instantaneous powers for demand, battery, SC, and its reference

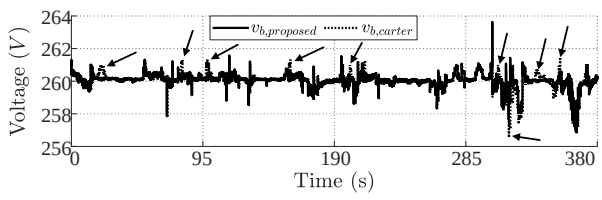

Figure 9. simulation results showing the proposed method and benchmark for the battery voltage

To assess the performance and health of batteries, HESS control algorithms can be validated through quantitative comparison using the overall RMS battery current. This method effectively measures the stress placed on a battery and is commonly employed to evaluate battery performance and condition [26]. The RMS value method determines the representative measure of the battery usage by calculating the RMS value of the current flowing through the battery over a specific time period.

The RMS battery current values for the selected portion of the medium section of the WLTP driving cycle were found to be 43.68 A and 42.92 A for the benchmark and proposed methods, respectively. This indicates a slight improvement of about 1%, which can be significant for complete and repeated driving cycles. Finally, another perspective on the voltage stability of the battery is to compare the voltage deviation using the formula in equation (18):

$$\mathrm{V}_{dv}(\%) = \frac{v_{\mathrm{b,\,max}} - v_{\mathrm{b,\,min}}}{v_{\mathrm{b,\,initial}}} \cdot 100\% \qquad (18)$$

Where $v_{b,max}$, $v_{b,min}$, and $v_{b,initial}$ are the maximum, minimum and initial voltage. The proposed improves the voltage deviation from 2.73% to about 2.57%.

5. CONCLUSION

In conclusion, this paper presented a semi-active SC/battery system model and designed a current PI regulator. A novel SC voltage reference was derived based on the energy conservation law, and a rule-based power follow strategy was developed incorporating the proposed method. The simulation results, comparing the benchmark and proposed methods, demonstrated several key findings.

Firstly, the proposed method, with the modified SC voltage reference, achieved a more dynamic SOC behaviour, this dynamic behaviour was particularly noticeable during certain periods of the driving cycle, where the proposed method effectively utilized the available energy for acceleration power, leading to improved performance. In addition, the proposed method significantly enhanced voltage stability, as evidenced by the absence of voltage spikes observed. Quantitative analysis using RMS battery current demonstrated a slight improvement of approximately 1% for the proposed method compared to the benchmark method. This improvement, although seemingly small, becomes significant when considering complete and repeated driving cycles. Finally, the voltage deviation analysis showed a reduction from 2.73% to approximately 2.57%.

Overall, the simulation results validate the effectiveness and benefits of the proposed method in terms of dynamic SOC behaviour, voltage stability, and battery current performance. The proposed method offers an enhanced EMS for semi-active SC/battery systems, thereby improving the overall efficiency and performance of electric vehicles.

ACKNOWLEDGMENT

The authors are thankful for the financial support through The Ministry of Higher Education under Universiti Teknologi Malaysia for the High-Tech Research Grant with vote number of Q.J130000.4623.00Q21 and

Professional Development Research University Grant with vote number of Q.J130000.21A2.07E30.

REFERENCES

[1] J. Loveday, "US EV adoption happening faster than anticipated, research shows," Teslarati, 2022. [Online]. Available: https://www.teslarati.com/us-ev-adoption-faster-anticipated. [Accessed: 30-Jun-2023].

[2] A. Albatayneh, M. N. Assaf, D. Alterman, and M. Jaradat, "Comparison of the Overall Energy Efficiency for Internal Combustion Engine Vehicles and Electric Vehicles," Environ. Clim. Technol., vol. 24, no. 1, pp. 669–680, 2020.

[3] U. N. E. Programme, "Supporting the global shift to electric mobility." [Online]. Available: https://www.unep.org/explore-topics/transport/what-we-do/electric-mobility/supporting-global-shift-electric-mobility. [Accessed: 30-Jun-2023].

[4] E. Wood, M. Alexander, and T. H. Bradley, "Investigation of battery end-of-life conditions for plug-in hybrid electric vehicles," J. Power Sources, vol. 196, no. 11, pp. 5147–5154, 2011.

[5] V. S. Vulusala G and S. Madichetty, "Application of superconducting magnetic energy storage in electrical power and energy systems: a review," Int. J. Energy Res., vol. 42, no. 2, pp. 358–368, 2018.

[6] I. Hadjipaschalis, A. Poullikkas, and V. Efthimiou, "Overview of current and future energy storage technologies for electric power applications," Renew. Sustain. Energy Rev., vol. 13, no. 6, pp. 1513–1522, 2009.

[7] Skeleton Technologies, "SkelMod 54V 277F supercapacitor module." [Online]. Available: https://www.skeletontech.com/en/supercapacitor-modules.

[8] J. Cao and A. Emadi, "A new battery/ultra-capacitor hybrid energy storage system for electric, hybrid and plug-in hybrid electric vehicles," 5th IEEE Veh. Power Propuls. Conf. VPPC '09, pp. 941–946, 2009.

[9] Z. Song, H. Hofmann, J. Li, X. Han, X. Zhang, and M. Ouyang, "A comparison study of different semi-active hybrid energy storage system topologies for electric vehicles," J. Power Sources, vol. 274, pp. 400–411, 2015.

[10] R. Xiong, H. Chen, C. Wang, and F. Sun, "Towards a smarter hybrid energy storage system based on battery and ultracapacitor - A critical review on topology and energy management," J. Clean. Prod., vol. 202, pp. 1228–1240, 2018.

[11] R. Carter, A. Cruden, and P. J. Hall, "Optimizing for efficiency or battery life in a battery/supercapacitor electric vehicle," IEEE Trans. Veh. Technol., vol. 61, no. 4, pp. 1526–1533, 2012.

[12] S. Pay and Y. Baghzouz, "Effectiveness of battery-supercapacitor combination in electric vehicles," 2003 IEEE Bol. PowerTech - Conf. Proc., vol. 3, pp. 728–733, 2003.

[13] F. R. Salmasi, "Control strategies for hybrid electric vehicles: Evolution, classification, comparison, and future trends," IEEE Trans. Veh. Technol., vol. 56, no. 5 I, pp. 2393–2404, 2007.

[14] Z. Song, H. Hofmann, J. Li, J. Hou, X. Han, and M. Ouyang, "Energy management strategies comparison for electric vehicles with hybrid energy storage system," Appl. Energy, vol. 134, pp. 321–331, 2014.

[15] Z. Lu and X. Zhang, "Composite Non-Linear Control of Hybrid Energy-Storage System in Electric Vehicle," Energies, vol. 15, no. 4, 2022.

[16] X. Zhang, Y. Wang, X. Yuan, Y. Shen, Z. Lu, and Z. Wang, "Adaptive Dynamic Surface Control with Disturbance Observers for Battery/Supercapacitor-based Hybrid Energy Sources in Electric Vehicles," IEEE Trans. Transp. Electrif., vol. PP, p. 1, 2022.

[17] Y. Hu, C. Chen, T. He, J. He, X. Guan, and B. Yang, "Proactive Power Management Scheme for Hybrid Electric Storage System in EVs: An MPC Method," IEEE Trans. Intell. Transp. Syst., vol. 21, no. 12, pp. 5246–5257, 2020.

[18] B. Hredzak, V. G. Agelidis, and M. Jang, "A model predictive control system for a hybrid battery-ultracapacitor power source," IEEE Trans. Power Electron., vol. 29, no. 3, pp. 1469–1479, 2014.

[19] C. Jia, J. Cui, W. Qiao, and L. Qu, "Real-Time Model Predictive Control for Battery-Supercapacitor Hybrid Energy Storage Systems Using Linear Parameter Varying Models," IEEE J. Emerg. Sel. Top. Power Electron., vol. 6777, no. c, pp. 1–1, 2021.

[20] J. Moreno, M. E. Ortúzar, and J. W. Dixon, "Energy-management system for a hybrid electric vehicle, using ultracapacitors and neural networks," IEEE Trans. Ind. Electron., vol. 53, no. 2, pp. 614–623, 2006.

[21] M. E. Choi, J. S. Lee, and S. W. Seo, "Real-time optimization for power management systems of a battery/supercapacitor hybrid energy storage system in electric vehicles," IEEE Trans. Veh. Technol., vol. 63, no. 8, pp. 3600–3611, 2014.

[22] M. I. Ramdan and A. F. Hawary, "Perodua Myvi parallel hybrid hydraulic passenger vehicle fuel economy simulation on Malaysia drive cycle, using rule-based control strategy," AIP Conf. Proc., vol. 2059, 2019.

[23] Y. Guan, Z. Q. Zhu, I. A. A. Afinowi, J. C. Mipo, and P. Farah, "Design of synchronous reluctance and permanent magnet synchronous reluctance machines for electric vehicle application," 2014 17th Int. Conf. Electr. Mach. Syst. ICEMS 2014, pp. 1853–1859, 2014.

[24] Y. Liao, H. Wang, M. Zhu, and A. Thomas, "Efficient Supercapacitor Energy Storage Using Conjugated Microporous Polymer Networks Synthesized from Buchwald–Hartwig Coupling," Adv. Mater., vol. 30, no. 12, pp. 1–10, 2018.

[25] R. W. Erickson and D. Maksimovic, Fundamentals of Power Electronics, 2nd edition, 2ed ed. Springer, 2004.

[26] P. J. Kollmeyer, M. Wootton, J. Reimers, D. F. Opila, H. Kurera, M. Kadakia, R. Gu, T. Stiene, E. Chemali, M. Wood, and A. Emadi, "Real-Time Control of a Full Scale Li-ion Battery and Li-ion Capacitor Hybrid Energy Storage System for a Plug-in Hybrid Vehicle," *IEEE Transactions on Industry Applications*, vol. 55, no. 4, pp. 4204-4214, 2019.